JOURNAL OF MATERIALS SCIENCE 3 (1968) 507–518

Cathodoluminescent Studies of Laser Quality GaAs

D. A. SHAW, P. R. THORNTON
School of Engineering Science, University College of North Wales, Bangor, Caerns, UK

Received 11 March 1968

Using an ion-pumped scanning electron microscope, cathodoluminescent (CL) studies of striations, dislocation-induced defects, and the doping behaviour of Te, Se, and Si in GaAs, have been carried out. The striations in heavily Te-doped Czochralski material were different from those previously reported in that they possessed a very regular spacing which agreed well with the growth/revolution of the ingot. They were studied as a function of temperature, excitation and position on the crystal face. It is thought that these bright striations in highly-doped material correspond to regions of decreased Te concentration in agreement with earlier work. However, infra-red studies of striations at lower concentrations have shown that the bright striations correspond to an increase in Te concentration. These results are consistent with earlier work relating CL efficiency to doping level. Studies of the dislocation-induced defects and their reactions with the striations in Te-doped material are all consistent with the formation of a Cottrell atmosphere at the dislocations at the expense of the immediate surrounding volume. Comparisons between Te-, Se-, and Si-doped material prepared by three different methods have revealed differences, especially in the case of Si where direct observation of its amphoteric nature were recorded.

1. Introduction

Cathodoluminescence, or electron-beam-induced photon emission, can now be used to study the microscopic properties of important electroluminescent materials. Recent studies of this type [1-3] using modified X-ray microanalysers have shown that the cathodoluminescent (CL) properties of Te-doped GaAs contain two types of localised defect. The inhomogeneities consist of "spots" or circular regions and "striations" or linear bands of varying signal. Careful microanalysis [4] on such striations in 5.2×10^{18} atom/cm^3 Te-doped material has shown that the dark regions correspond to an increase in Te concentration. The reported geometries of the striations vary considerably and the separation between the striations did not correlate in a simple way with the growth per revolution in the Czochralski-grown material [2, 5, 6]. Etching techniques have established that the spot defects occur at the sites of emergent edge dislocations [2, 3]. These initial studies have established many properties of the localised inhomogeneities in laser quality GaAs. However, several questions remain unanswered, and some of the assumptions used to interpret the observations need confirmation if they are to be applied over a wide range of dopant concentration. To be specific, we can quote the following points. (i) Both the striations and the dislocation-induced defects exhibit a wide range of CL behaviour, the details of which have not been completely catalogued or explained. (ii) The exact relationship between the contrast observed at the two types of defect has to be established. (iii) No observations have been reported in material doped with Se and Si, which are also commonly used in laser fabrication. The observations reported in this paper were made to examine these and other questions.

Using an ion-pumped scanning electron microscope (SEM) we have studied these CL spot and striation defects over a wide range of dopant concentration, and have shown that on relatively lightly-doped material, the striation

dark regions correspond to a decrease in Te concentration in contrast to previous reports [3]. The majority of the observations presented here were made on striations which had very regular spacings, which agreed well with the growth/revolution of the Czochralski-grown crystal. The peak signal from the striations was compared with the background signal as a function of temperature, excitation level, and position on the crystal slice. A physical model which also reconciles all the available data is proposed to explain the origin and properties of these striations. The structure of the spot defects was investigated by observing their interactions with the striations. From these results a model of the defect structure is proposed, which is qualitatively consistent with all the observations. These studies were extended to include material that had been doped with Se and with Si. Major differences in the microscopic behaviour of the dopants with the defects were observed and, in the case of Si, direct observations of its amphoteric character were recorded.

2. Experimental

A modified Cambridge Instrument Company scanning electron microscope was used with an uncooled S1 photomultiplier to detect the CL emission. This was mounted to allow line-of-sight collection of the radiation with a collection angle of ~0.25 steradian. A beam energy of 20 keV was used with a beam current in the range 5×10^{-10} to 10^{-6}A. The specimen could be cooled using a stage based on a miniature Joule-Thomson liquefier [7]. The beam current could be measured by means of a Faraday cage attached to the specimen stage. The usual arrangements for obtaining micrographs of the specimen surface and of the charge collection currents generated in the laser specimens by the electron beam were also used.

A standard optical microscope was modified for the infra-red transmission studies. The light source used was a tungsten lamp in conjunction with a Kodak Wratten Filter No. 87. Infra-red Polaroid film was used for photography. The GaAs slices were etch-polished in a 10% bromine in methyl alcohol solution [8] prior to examination. Laser specimens were prepared from Static Freeze, Horizontal Bridgman and Czochralski material, doped with Te, Se or Si. The junctions were prepared by Zn-diffusion using two different diffusion schedules. The first schedule consisted of heating the specimen at 1100° C for 15 min with no As overpressure. The second was carried out at 850° C for 4 h in an overpressure of As.

3. Observations and Results

3.1. Studies of the Striations

In fig. 1 we show the striation pattern observed

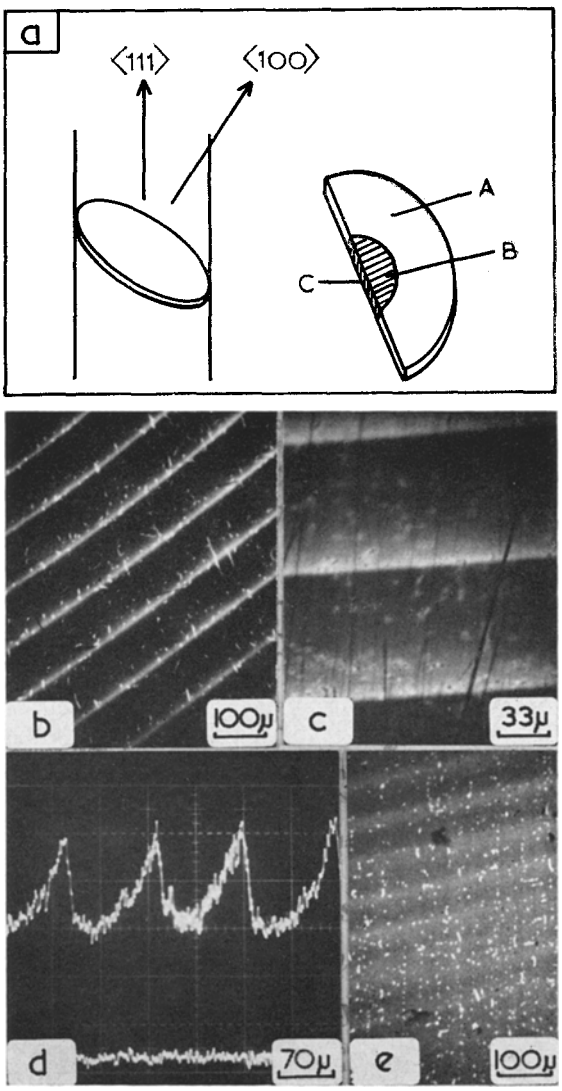

Figure 1 The important features of the regular striations in a crystal Te-doped to 4×10^{18} atom/cm^3. Fig. 1a shows the position of the slice examined and the regions of differing behaviour. Fig. 1b is a CL micrograph showing the appearance of the striations and dislocation-induced defects in region A, whilst (e) shows the virtual disappearance of the striations in the central regions B and C. Fig. 1c shows the sharp and diffuse edges of the striations whereas (d) shows the CL signal along a line perpendicular to the striations, again demonstrating the steep and slow edges of the striations.

on an undiffused, ⟨100⟩ oriented slice cut from a ⟨111⟩ oriented Czochralski-grown crystal, see fig. 1a. Fig. 1b shows a CL micrograph of the slice taken in the area A of the slice and illustrates both types of defect. Fig. 1c shows a higher magnification view of part of fig. 1b. Two features of these striations should be stressed. One is their very regular nature, i.e. they appear as regular bands of high intensity about 20 μm wide. The second feature is that the bands have one sharp edge and one diffuse edge. This behaviour is more clearly seen in fig. 1d which shows the signal variation taken along a line perpendicular to the striations. This type of behaviour was observed over all the outer region, A, of the cut slice shown schematically in fig. 1a, and the steep edges all faced in the same direction. The striations in the central shaded region, B, of the slice have a different appearance, fig. 1e. Here the sharp edges have disappeared and the striations have largely merged into the background. The same pattern of behaviour was also observed along the cut edge of the specimen, i.e. the striations became ill-defined in the central region, C, fig. 1a.

By accurately calibrating the magnification of the SEM we were able to measure the separation of the regular striations as 120 $\pm$ 5 μm. From the known crystal pulling and rotation rates we calculated that the separation on this ⟨100⟩ orientated slice should be 123 μm. Regular striations such as these were observed in only two Te-doped Czochralski crystals. Irregular, ill-defined striations were observed in other ingots in accord with previous observations [2, 3]. We could not locate such variations in undoped Czochralski material or in Te- and Se-doped Horizontal Bridgman material.

Casey [3] has assumed that the bright regions in the striation patterns correspond to a decrease in Te-concentration compared to the bulk over a wide range of Te-concentration ($\sim 10^{17}$ to $\sim 10^{19}$ atom/cm^3). As this assumption appeared to be at variance with the known variation of CL efficiency as a function of dopant level [9] (see below) we tested this assumption by examining the striation behaviour in a lightly-doped (3×10^{17} atom/cm) pulled crystal. Some results are shown in fig. 2. The striations appear essentially as dark bands on a lighter background, see figs. 2a, b, approximately 120 μm apart. This slice was lapped and etch-polished in order to observe the infra-red transmission pattern. Fig. 2c shows the striations, as observed by infra-red transmission, as dark bands. The dark dots are small markers of "Aquadag" used in order to relate the infra-red absorption pattern to the CL micrograph. This is shown in fig. 2b.

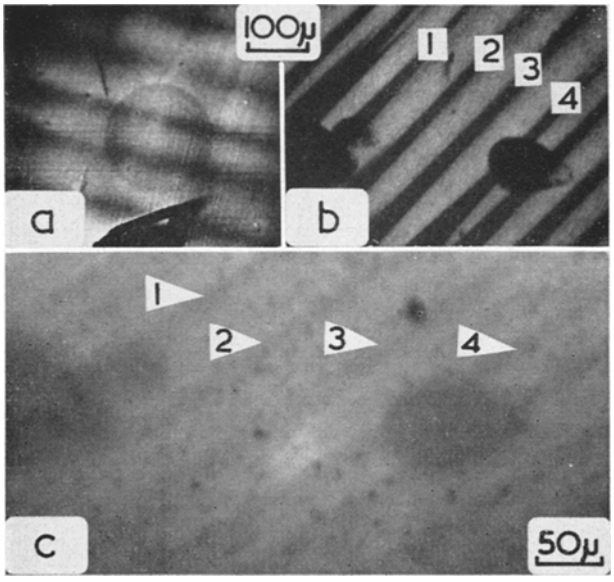

Figure 2 Striations on a slice Te-doped to 3×10^{17} atom/cm^3. Fig. 2a is a CL micrograph showing the appearance of the striations as dark bands on a lighter background. Fig. 2b shows a CL micrograph of the area thinned for infra-red transmission and (c) shows the striations as seen by infra-red transmission. Figs. 2b and c can be related using the marker dots of "Aquadag".

It can be seen that the dark striations of low CL efficiency correspond to lines of higher absorption coefficient.

To study the origins of these differing signal levels further, they were measured as a function of temperature and excitation level, i.e. beam current. These data are shown in figs. 3a, b. As the temperature of the specimen was reduced from 300 to 130° K, the peak and background signals increased in the same manner. If the signals are measured at 130° K as a function of excitation (over four decades) the variation from the peak and background is identical. The observations indicate that the CL intensity varies as $T^{-1.64 \pm 0.15}$ and $I_B^{0.96 \pm 0.1}$, both in the bright regions and in the background.

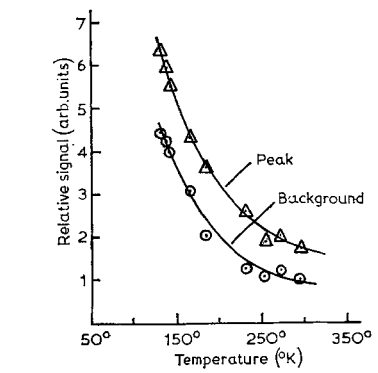

(a)

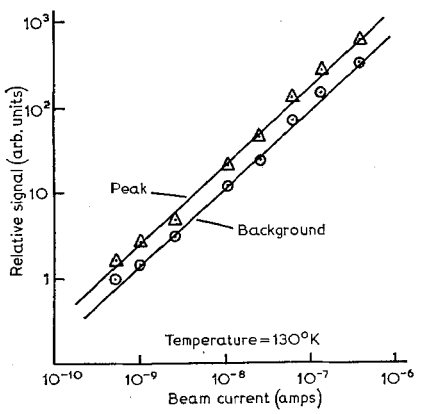

(b)

Figure 3 (a) shows the variation of CL signal with temperature for both the peak signal and background signal on a slice Te-doped to 4×10^{18} atom/cm^3. Fig. 3b shows the variation of these signals with beam current at a temperature of 130° K on the same specimen as above.

3.2. Studies of the "Spot" Defects

Initial experiments confirmed previous work relating the occurrence of etch pits to the luminescent spots [2, 3]. A straightforward method of doing this has been reported elsewhere [10]. Often these defects consist of a dark core surrounded by a bright halo but the actual geometry depends on the angle of emergence of the dislocation. This is illustrated in figs. 4a, b. The relative intensity of the bright halo varies from specimen to specimen, and in some cases the halo is almost entirely absent, the defect then consists essentially of a dark, non-luminescent centre; see fig. 4c. Fig. 4d shows an intermediate situation in which the defects have "dead spots" in the centres and large diameter, but weak halos.

Our observations suggest that there is no spatial correlation between the spot defects and the striations; however, the formation of each type of defect is not independent of the other. Fig. 4e shows a CL micrograph demonstrating the interdependence. This clearly shows that spot defects occurring in the immediate vicinity of a bright striation possess a much brighter halo than other spot defects on the specimen. This effect was checked using a signal level discrimination device which allows contours of equal CL signal to be recorded. This effect was also observed on specimens exhibiting irregular striations.

Fig. 4c shows the dislocation-induced defects interacting with the dark striations and essentially reducing the local striation width. These spot defects have a fairly general occurrence. We have observed them in Te-doped Czochralski- and Static-Freeze-prepared crystals and, to a lesser extent, in Se-doped Horizontal Bridgman material. We were unable to detect such variations in undoped Czochralski material.

3.3. Observations on Laser Faces

In this paper we shall limit the discussion to the CL properties of the bulk regions (see section 5).

Fig. 5 shows CL micrographs of the optically polished faces of Te-doped GaAs lasers*. In these micrographs the junction, indicated by J, is located on the left hand side of the observed signal; little or no signal is observed from the highly-doped p-type side of the device. The only feature common to these micrographs is the degradation of CL signal in the neighbourhood of surface scratches and microcracks. This

*The orientation of these lasers with respect to the crystallographic axes is unknown.

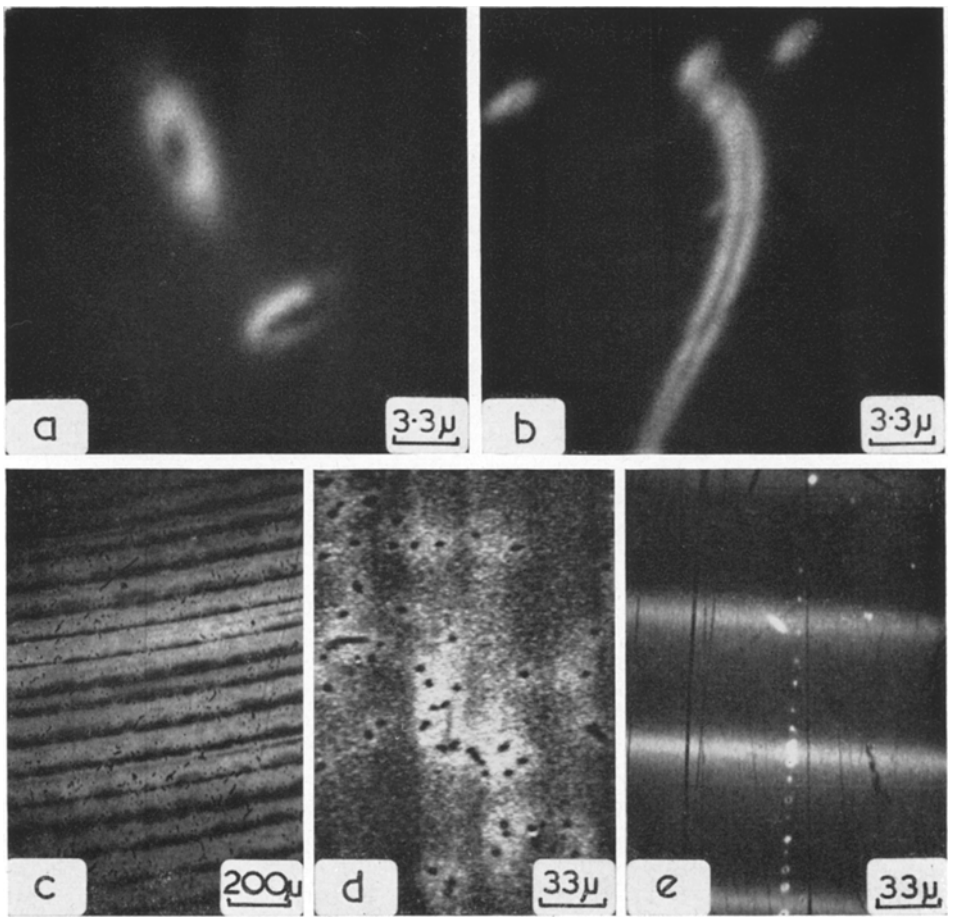

Figure 4 The important features of the dislocation-induced defects. Fig. 4a shows the effect produced by a dislocation essentially perpendicular to the surface whereas (b) shows one almost lying along the surface. Fig. 4c shows the dislocation-induced defects interacting with dark striations whilst (e) shows their interaction with light striations. Fig. 4d shows dislocation-induced defects with weak, large area halos.

effect has been observed before [2, 3] and will not be discussed further here. Fig. 5a shows the CL signal obtained from a Te-doped laser which had been prepared by the first diffusion schedule described above (no As overpressure). In addition to a band of high CL signal along the junction, there are roughly circular regions of high efficiency which are unrelated to the junction geometry and which are centred on spots of low CL signal. Often the efficient regions extend far enough to join together to form complex shapes (see figs. 5b, c). These regions are associated with the dislocation structure of the crystal used. Only a fraction of the dislocation density causes these regions. To determine the cause in more detail we compared CL maps with the surface structure revealed by etching [11]. The pertinent results are shown in fig. 6. Fig. 6a shows the CL map from one of the "linear" regions that are sometimes observed (see fig. 5). Fig. 6b shows the surface of the same area after etching. The etching reveals that there is a defect present which has the superficial characteristics of a twinned region. The etching also shows that the outline of regions of high CL often coincide with the boundary between regions of different etch rate. This is shown more emphatically in figs. 6c, d. Finally in figs. 6e and f one of the large circular regions of high CL efficiency is shown in relation to the local defect distribution. It is apparent that the circular nature of the CL distribution can only be related very loosely to

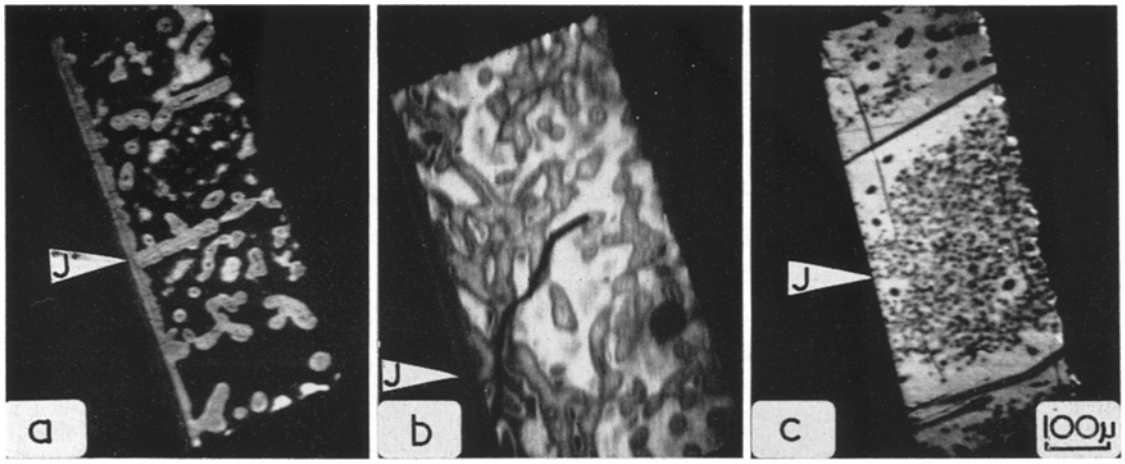

Figure 5 CL micrographs of one optically polished face of each of three Te-doped lasers made from Horizontal Bridgman material. Those shown in (a) and (b) were prepared by the first diffusion schedule (no As overpressure) whereas that shown in (c) was prepared by the second schedule (with As overpressure). The markers indicate the junction positions.

the local defect content. These micrographs (figs. 5 and 6) are typical of all the faces examined of devices made with Te-doped material. The vast majority of such faces showed gross local variations in CL efficiency although the detailed appearance varied considerably. For example, figs. 7a, b show two faces in which the patterns differ from those described so far in that the local variations are smaller in extent and there is a clear indication of an interaction between the dopant (Zn) used to form the junction, and atoms already present in the material. This interaction appears to occur only when there is no overpressure of As and takes the form of strong and/or weak CL bands ahead of the p-n junction, i.e. on the n-type side of the junction.

We have made a limited comparison with lasers made in Se-doped material. Figs. 7c, d contain the salient points. The CL emission is much more uniform. Fig. 7c shows a typical laser made in Se-doped material while Fig. 7d shows a poor one. The interaction with dislocations is far less prevalent. In fact it is often difficult to find any evidence of localised changes in CL near dislocations. By etching we established that, although there were microscopic variations in CL efficiency, these are no more prevalent near dislocation cores than elsewhere. In Se-doped material the microscopic variations take the form of small ($\sim$2 μm) dead spots of unknown origin. Again we observe CL banding ahead of the junction in lasers diffused with no As overpressure.

Finally, figs. 7e, f show the CL maps of lasers prepared from Si-doped material. The first laser has a layer of n-type material ahead of the junction which gives an intense signal about 50 μm wide. This behaviour is characteristic of both faces of the laser. It is also characteristic of a laser prepared by the second diffusion schedule, fig. 7f. In this case the only difference is that the intense layer is somewhat wider. It should be stressed here that these variations are not related to localised defects but appear to be a bulk effect related to the geometry of the diffusion. As with the Se-doped material the effect of dislocations on the CL behaviour is minimal.

4. Discussion of the Results

4.1. The Striation-Formation

The regular striations observed in the highly-doped material differ from the irregular striations previously reported [1, 2, 5, 6]. In addition, the striation spacing agrees well with the crystal growth per revolution. The measurements of the CL efficiency in the striations and in the background as a function of temperature and excitation level strongly suggest a common origin and that they differ only in degree. This is in agreement with results obtained by microanalysis [4] which showed that in highly-doped material the bright striations correspond to regions of reduced Te concentration. We suggest that the temperature and excitation dependence of the bright region and the background signal

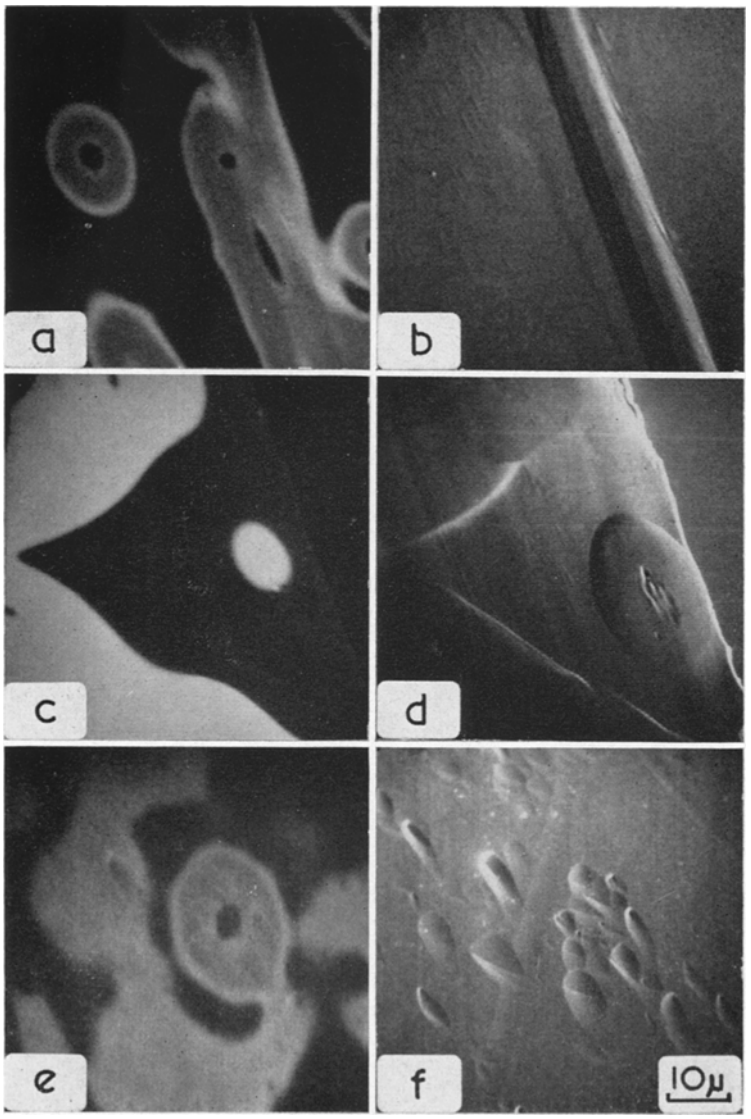

Figure 6 The results of etching studies carried out on the laser shown in fig. 5a. Figs. (a), (c), (e) are CL micrographs whereas (b), (d) and (f) are the corresponding topographic micrographs showing the structure as revealed by etching See text for details.

levels are indicative of "band-edge" transitions involving different concentrations of Te-atoms. These variations could be introduced during the crystal growth in the following way.

If random changes in temperature occur at the growth interface, or if supercooling takes place, the striations formed will be irregular [2, 5, 6]. However, regular variations in temperature such as those due to a lateral gradient in a rotating crystal will lead to regular striations. The quantitative agreement between the predicted and measured striation separation supports this idea. The various striation geometries reported can be reconciled by assuming a curved rather than a planar growth interface. Such interfaces have been observed in Czochralski crystals [5]. Under these conditions the striation geometry will depend on the curvature, separation and regularity of the variations in doping level. If the separation is large and the curvature small, it is possible to obtain sections which show no striations. Such sections have been observed

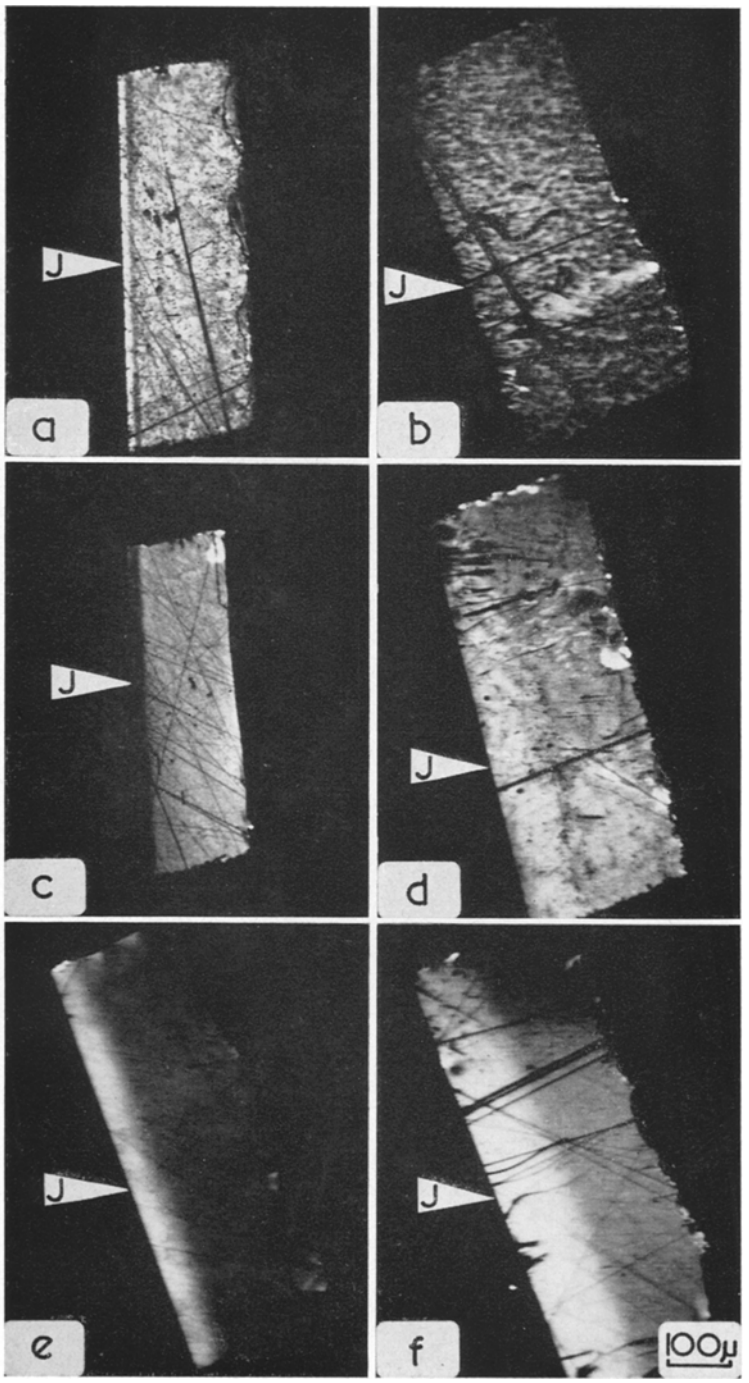

Figure 7 CL micrographs of the optically polished faces of lasers prepared from differing materials. Figs. 7a, b are lasers prepared from Te-doped Static Freeze material; (a) by the first diffusion schedule (no As overpressure) and (b) by the second schedule. Figs. (c) and (d) are lasers prepared from Se-doped Horizontal Bridgman material; (c) by the first schedule and (d) by the second. Figs. (e) and (f) are lasers made in Si-doped Horizontal Bridgman material; (e) by the first schedule, and (f) by the second one. The markers indicate the junction positions. The details are discussed in the text.

in the present work. With a high curvature and small separation, concentric circles may be observed [3, 5, 12]. If the section examined is not perpendicular to the growth axis then parallel bands may be seen [2, 5, and the present work]. The inclination of the growth interface with respect to the upper face of the slice explains the sharp and diffuse edges of the striations. Fig. 8 shows the situation schematically. The

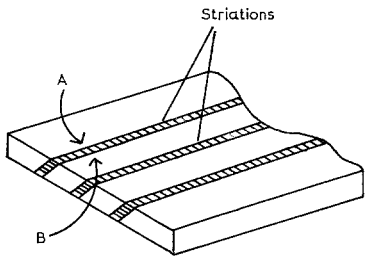

Figure 8 Schematic diagram of the slice examined showing the striations intersecting the surface at an angle, and the positions of the sharp and diffuse striation edges.

finite penetration of the electron beam will lead to a slow decay of the signal at edge A of the striation, but a sharp edge will be observed at B. The variability of the sharpness of the edges, cf fig. 1c and fig. 4e, is explained by the variation in inclination of the striations due to the curvature of the growth interface. The virtual disappearance of the striations towards the centre of the slice is predictable, as the centre of the ingot would not be subjected to temperature variations as large as those at the outer edges in the presence of a lateral temperature gradient.

4.2. The Relationship Between the Striation Characteristics and the Variations in Dopant Concentration

We know from Cusano's work [9] relating the CL efficiency to dopant concentration, that the efficiency increases with increasing Te-dopant concentration up to 2×10^{18} atom/cm^3 which corresponds to the peak efficiency. Further increase in the dopant level results in a reduction in CL efficiency. Wittry's observations [4] in highly-doped material ($\sim 5.2 \times 10^{18}$ atom/cm^3) that the regions of high CL efficiency correspond to a decrease in Te-concentration compared to the bulk are in agreement with Cusano's data. Our observations on lightly-doped material ($\sim 3 \times 10^{17}$ atom/cm^3) suggest that the bright regions correspond to regions of higher than average dopant concentration. At these concentrations X-ray microanalysis is not possible and we had to relate variations in CL efficiency to variations in infra-red absorption. We have shown that in lightly-doped material regions of low CL efficiency correspond to regions of higher than average absorption. It is known [13] that, over the range of 2×10^{17} to 5×10^{18} atom/cm^3, the absorption coefficient increases monotonically as the n-type dopant concentration decreases. Therefore the regions of low CL efficiency correspond to regions of lower than average dopant concentration. This result is again consistent with Cusano's data but contradicts the assumption made by Casey [3] who extrapolated Wittry's conclusion to dopant levels $< 2 \times 10^{18}$ atom/cm^3.

Finally we should note that using Cusano's data and the observations presented here it is possible to estimate the variations in dopant level in the crystals studied. We estimate that the variations lie between 10 and 40% at dopant levels of 4×10^{18} atom/cm^3. The implication is that by extending Cusano's data and using more refined detector systems it should be possible to study variations in dopant concentrations down to the low 10^{15} atom/cm^3 range.

4.3. The Contrast Features Observed at the Dislocation-Induced Defects

The most obvious model to explain the contrast observed at the dislocation-induced defects is to assume that a Cottrell atmosphere [14] of Te-atoms is formed around the dislocations. This idea has already been suggested [2] and is supported by several facts. The absence of these defects in undoped material suggests that the contrast observed is not an intrinsic property of the dislocations themselves. The correlation between the occurrence of these defects and the presence of edge, rather than screw, dislocations [2] indicates the importance of tensile or compressive strain rather than sheer strain. It should also be noted that, of the three dopants used in this work, Te has the largest misfit energy. Te is $\sim 12\%$ [15] larger than the As atom, whereas the Se atom is 3% smaller than the As atom and Si is $\sim 7\%$ smaller than Ga. Only in Te-doped materials have large, localised variations in CL efficiency been observed at dislocations. In Se-doped materials the effect is much less pronounced and in Si-doped materials there are complications due to its amphoteric

nature which may hinder the observation of the effect (see below). The observations reported here of the interactions between the dislocation-induced defects and the striations also support the idea that variations in Te-content are important to both. For example, in the crystal shown in fig. 4e (Te-doping level 4×10^{18} atom/cm^3), the brightest halos occur in the bright regions of the striations and are brighter than these regions. The implication is that the dislocation "core" partially denudes the halo region leading to increased CL. The same argument applies to the crystal shown in fig. 4c which is also highly doped.

It should be stressed that reports of the contrast at dislocation-induced defects vary considerably. For example, Casey [3] reports halos occurring in striations which differ little in intensity from the bright striation regions. All the observed variations can be explained by assuming a Te atmosphere at the dislocations and by assuming that Cusano's data are applicable in this situation. Fig. 9 shows how the observed contrast features can be explained if it is assumed that the diffusion of Te towards the core of the dislocation reduces the concentration in the adjacent volume. Contrast patterns of the four types shown in fig. 9 have been observed.

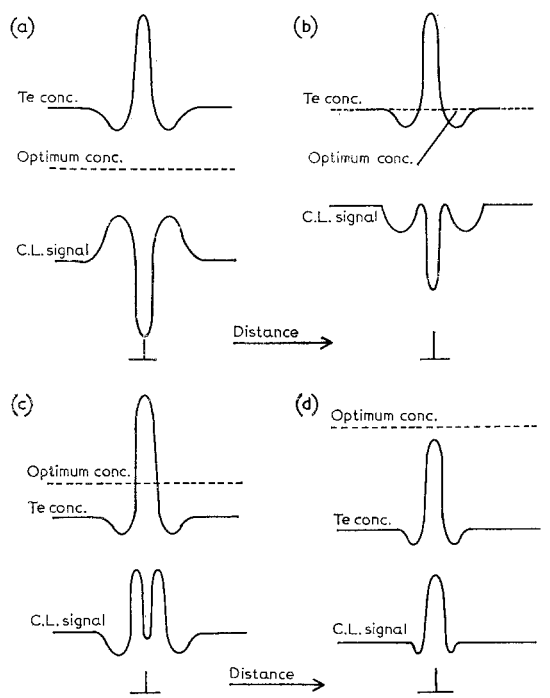

Figure 9 Schematic diagrams of the redistribution of Te occurring at dislocations and the corresponding CL signal when (a) the optimum concentration is below the bulk concentration; (b) the optimum concentration equals the bulk level; (c) the optimum level is above the bulk level but below the peak level; and (d) the optimum level is above the peak level.

4.4. CL Contrast Observed on Polished Laser Faces

It is convenient to consider the lasers made in Si-doped material first as we could not obtain evidence of interactions between this dopant and the defect structure of the material. The main difference between these lasers and those made in Te- and Se-doped GaAs is the intensity and extent of the band of high CL on the n-type side of the junction in the Si-doped diodes. It is known that Si is amphoteric [16]. This impurity is normally incorporated into the Ga sub-lattice as a donor, but above concentrations of $\sim 10^{18}$ atom/cm^3 a significant fraction are incorporated as acceptors on the As sublattice [16]. We assume that radiative recombination occurs through Si-atoms in the donor state and that the CL efficiency thus depends on the concentration of Si-atoms in this state [9]. We propose that the diffusion of Zn into the Si-doped material increases the proportion of Si atoms in the donor state in the junction region, and that this leads to the observed increase in CL efficiency. Such an interaction due to the presence of other impurities has been discussed previously [17]. For example, tracer experiments on Cu [18] and Mn [19] have shown that a Zn diffusion can affect the distribution of these impurities up to 100 μm ahead of the junction in a manner which depends on the diffusion schedule and the As overpressure. The above model only holds as long as (i) the Si concentration prior to diffusion is such that a fraction of the Si-atoms are in the acceptor state, i.e. the total concentration is $\geqslant 10^{18}$ atom/cm^3, and (ii) the donor concentration prior to diffusion is less than that which gives peak CL efficiency, i.e. less than $\sim 2 \times 10^{18}$ atom/cm^3. The width of the intense region appears to depend on the diffusion conditions and/or the As overpressure. The trend of this dependence is that expected from the fact that the As pressure was greater in the slow diffusion which gives the wider band. (Compare the behaviour of Cu and Mn referred to above.)

The Se-doped lasers give a much more uniform behaviour than the Te-doped devices. In only a small fraction of the Se-doped devices are

localised variations in CL efficiency observed. These take the form of small dead spots about 2 μm in diameter. We have no indication of the cause of these at present. In both the Te- and Se-doped materials there appears to be an interaction between the Zn used to form the p-n junction and the dopant atoms near to the junction on the n-type side when no As over-pressure is used during the diffusion. It is probable that the observed CL behaviour results because this interaction alters either the number of or the manner in which the Te and Se atoms can take part in the radiative recombination. We do not know at present the extent to which Zn and Te and Se interact. As a result we cannot offer a detailed explanation, nor can we exclude the possibility that the behaviour is due to changes in wavelength of the emitted light which lead to contrast because of the wavelength dependence of the system detectivity.

The apparent lack of detailed correlation between the local variations in CL efficiency and the dislocation structure is consistent with previous studies of the voltage distribution and photo-conductivity in regions containing crystal mosaic [20]. These studies showed that, in regions of crystal containing subgrain boundaries and twins, the diffusion of impurities into or out of the crystal was enhanced by the presence of defects on a macroscopic scale, but did not follow the microscopic location of the defects. This behaviour would explain the observations of CL reported here. If the relevant dopant behaved thus, the localised variations would follow the general shape of the defect structure, but the microscopic CL behaviour, as revealed on any one surface cutting across this structure, would not correlate in detail with the defect structure, as it would depend to some extent on the defect structure above and below this surface.

5. Summary and Conclusions

The observations on the regular striations are all consistent with the idea that they are formed at a curved growth interface and that they consist of Te concentration variations. These variations are induced by regular temperature fluctuations such as those in a crystal rotating in a lateral temperature gradient.This model also correlates previous observations on heavily-doped samples. In lightly-doped material, the dark regions correspond to a reduction in Te concentration, whereas the reverse is true at high doping level, $> 2 \times 10^{18}$ atom/cm^3. This agrees with previous work relating CL efficiency to doping level.

The results on the dislocation-induced contrast are all consistent with the formation of a Cottrell impurity atmosphere at the dislocation core at the expense of the immediately surrounding volume. This model predicts various CL patterns, all of which have been observed. The observed interactions between the striations and the dislocation-induced contrast supports the above model.

Comparisons between the doping behaviour of Te, Se, and Si have revealed macroscopic differences. Whereas gross CL contrast is associated with dislocation structure in Te-doped material, this is not so frequent nor so severe in Se-doped material. Observations of Si-doped specimens have revealed direct evidence of its amphoteric nature.

Further work is to be carried out to relate the CL detail to device properties in the case of the laser specimens. It is planned to run the lasers in both the non-lasing and lasing modes in the SEM at $\sim$100° K and to use a modulated electron beam in order to investigate the variation in efficiency across the laser faces and to relate this to the properties of the starting material etc [21].

Acknowledgements

We should like to thank Mr C. Gooch, Mr M. Rowlands and Dr S. Bass of SERL, Baldock, Herts, for the GaAs lasers and slices. Also, the financial support given by the Science Research Council and CVD is gratefully acknowledged. This paper is published by permission of the Ministry of Defence (Navy Department).

References

1. D. B. WITTRY and D. F. KYSER, *J. Appl. Phys.* **35** (1964) 2439.
2. *Idem*, "The Electron Microprobe Conference" (Electrochem. Soc., Washington, 1964) p. 691.
3. H. C. CASEY, *J. Electrochem. Soc.* **114** (1967) 153.
4. D. B. WITTRY, *Appl. Phys. Lett.* **8** (1966) 142.
5. C. Z. LEMAY, *J. Appl. Phys.* **34** (1963) 439.
6. G. R. CRONIN, G. B. LARRABEE, and J. F. OSBORNE, *J. Electrochem. Soc.* **113** (1966) 292.
7. R. C. WAYTE and P. R. THORNTON, *J. Sci. Instr.* **44** (1967) 806.
8. M. V. SULLIVAN and G. A. KOLB, *J. Electrochem. Soc.* **110** (1963) 585.
9. D. A. CUSANO, *Solid State Communs.* **2** (1964) 353.
10. D. A. SHAW, D. V. SULWAY, R. C. WAYTE, and P. R. THORNTON, *J. Appl. Phys.* **38** (1967) 887.

11. M. S. ABRAHAMS and C. J. BUIOCCHI, *J. Appl. Phys.* **36** (1965) 2855.
12. E. S. MEIERAN, *J. Appl. Phys.* **36** (1965) 2544.
13. R. HUNSPERGER and J. BALLANTYNE, *Appl. Phys. Lett.* **10** (1967) 130.
14. A. H. COTTRELL and B. A. BILBY, *Proc. Phys. Soc.* **A62** (1949) 49.
15. L. PAULING, "The Nature of the Chemical Bond" (Cornell University Press, 1939).
16. J. M. WHELAN, J. D. STRUTHERS, and J. A. DITZENBURGER, Conference on Semiconductor Physics, Prague (1960) p. 943.
17. R. L. LONGINI and R. F. GREENE, *Phys. Rev.* **102** (1956) 992.
18. G. B. LARRABEE and J. F. OSBORNE, *J. Electrochem. Soc.* **113** (1966) 564.
19. R. F. PEART, K. WEISER, J. WOODALL, and R. FERN, *Appl. Phys. Lett.* **9** (1966) 200.
20. P. R. THORNTON, M. J. CULPIN, I. W. DRUMMOND, *Solid State Electronics* **6** (1963) 532.
21. P. R. THORNTON, "Scanning Electron Microscopy" (Chapman and Hall, London, 1968).